Available online at www.sciencedirect.com
SCIENCE DIRECT
Biomaterials 27 (2006) 3817–3824
Biomaterials
www.elsevier.com/locate/biomaterials

Combinatorial screen of the effect of surface energy on fibronectin-mediated osteoblast adhesion, spreading and proliferation ☆

Scott B. Kennedy[a,b], Newell R. Washburn[a,c], Carl George Simon Jr.[a,*], Eric J. Amis[a]

[a]*Polymers Division, National Institute of Standards & Technology, 100 Bureau Drive, Gaithersburg, MD 20899-8545, USA*
[b]*Department of Chemistry and Physics, Anderson University, Anderson, IN 46012 USA*
[c]*Departments of Chemistry and Biomedical Engineering, Carnegie Mellon University, Pittsburgh, PA 15213, USA*

Received 4 January 2006; accepted 24 February 2006
Available online 24 March 2006

Abstract

In order to accelerate tissue-engineering research, a combinatorial approach for investigating the effect of surface energy on cell response has been developed. Surface energy is a fundamental material property that can influence cell behavior. Gradients in surface energy were created by using an automated stage to decelerate a glass slide coated with a self-assembled monolayer (SAM, *n*-octyldimethylchlorosilane) beneath a UV lamp such that the SAM is exposed to the UV-light in a graded fashion. UV exposure causes oxidation of the SAM such that a longer exposure correlates with increased hydrophilicity. This approach yielded substrates having a linear gradient in surface energy ranging from 23 to 62 mN/m (water contact angles ranging from 25° to 95°). Using the gradient specimen approach enables all surface energies from 23 to 60 mN/m to be screened on each slide. Before cell culture, surface energy gradients were coated with fibronectin to allow a study of the effect of surface energy on fibronectin-mediated cell response. Cells were seeded on the fibronectin-coated gradients and adhesion, spreading and proliferation were assessed with automated fluorescence microscopy. Surface energy did not affect initial cell adhesion at 8 h. However, the rate of proliferation was linearly dependent on surface energy and increased with increasing hydrophobicity. Cell spread area was unaffected by changes in surface energy over the majority of the gradient although cells were significantly smaller on the most hydrophilic region. These results show that fibronectin-mediated cell spreading and proliferation are dependent on surface energy and establish a new combinatorial approach for screening cell response to changes in surface energy.

Keywords: Cell adhesion; Cell proliferation; Cell spreading; Osteoblast; Self-assembly; Surface energy

1. Introduction

Despite a 4.5 billion dollar investment in tissue-engineering research, a profitable product has not yet come to market [1,2]. One cause for this lack of success is the slow pace of research. Traditional research involves preparing samples one at a time for characterization and testing. Combinatorial methods lower the *cost* of experimentation by reducing the amount of time and material required for experiments [3]. This is done by creating libraries containing many specimens in one sample in the form of gradients or arrays. Combinatorial approaches have been very useful for pharmaceutical research [4,5] and their utility in materials science and biomaterials research is also becoming apparent [6–11].

An understanding of cell–material interactions can help in the design of tissue-engineered medical products. Material properties such as surface energy [12], modulus [13], crystallinity [10], surface roughness [14] and surface chemistry [15] can influence cell response to biomaterials. In the current study we focus on surface energy because surface energy is a fundamental material property that can influence cell behavior and biomaterial performance [12,16–28].

For instance, van der Valk et al. [12] observed that a mouse fibroblast cell line was better spread during culture

☆ This article, a contribution of National Institute of Standards and Technology, is not subject to US copyright.

*Corresponding author. Tel.: +1 301 975 8574; fax: +1 301 975 4977.
E-mail address: carl.simon@nist.gov (C.G. Simon Jr.).

0142-9612/$ - see front matter © 2006 Elsevier Ltd. All rights reserved.
doi:10.1016/j.biomaterials.2006.02.044

on hydrophilic surfaces than on hydrophobic surfaces. In a study by van Wachem et al. [16], human endothelial cell adhesion was best on surfaces with intermediate surface energies. Schakenraad et al. [17] found that the rate of growth for primary human fibroblasts increased with increasing hydrophobicity. These results and others support the thesis that surface energy can affect cell response to a material [12,16–28]. In order to help accelerate tissue-engineering research, we have developed a combinatorial approach for screening the effect of surface energy on cell function.

Linear gradients in surface energy were created on glass slides [29]. Self-assembled monolayers (SAM) made from *n*-octyldimethylchlorosilane were assembled on glass slides and the SAM-coated slides were placed on a motorized stage beneath a UV lamp. A gradient in UV exposure time was obtained by decelerating the motion of the stage. The gradient in UV exposure time created a gradient in surface energy across the slide by causing differential amounts of ozonolysis of the *n*-octyldimethylchlorosilane SAM. Ozonolysis causes oxidation of the hydrocarbon chains in the SAM and a more hydrophilic surface [30]. Gradients that ranged in water contact angle from 25° to 95° were created on a single slide. In order to focus on cell responses that were mediated by fibronectin, the surface energy gradients were pre-coated with fibronectin prior to cell seeding. Fibronectin is one of the primary extracellular matrix proteins that adsorbs to implanted materials and its adsorption can influence cell response [15,31,32]. Cells were cultured on the fibronectin-coated gradients and automated fluorescence microscopy was used to assess adhesion, spreading and proliferation.

2. Materials and methods

2.1. Preparation of self-assembled monolayers

Glass microscope slides were rinsed with ethanol, blown dry with nitrogen and exposed to UV radiation for 15 min to create a clean hydroxide surface layer. Slides were then rinsed with toluene and immersed in a 2.5% (by mass) solution of *n*-octyldimethylchlorosilane (Gelest, Inc., Morrisville, PA) in toluene. After 24 h, slides were rinsed with toluene, blown dry with nitrogen, and incubated at 120 °C under vacuum for 24 h. This process creates a hydrophobic SAM on the slides. Slides with SAMs were stored under vacuum at room temperature.

2.2. Preparation of surface energy gradient

Slides with SAMs were placed on a motorized stage below a UV lamp [29] with a 190 nm UV wand housed in an aluminum casing with a slit aperture 2 mm wide. Immediately upon lowering the lamp housing to within 0.2 mm of the slide surface, the motorized stage was set in motion. A gradient in UV exposure time was obtained by decelerating the motion of the stage. The gradient in UV exposure time created a gradient in surface energy across the slide by causing differential amounts of ozonolysis of the hydrocarbon present in the *n*-octyldimethylchlorosilane [30]. Ozonolysis of the SAMs converts the CH_3 terminated layer into OH and COOH terminated species. Long exposure time correlates with high surface energy, increased hydrophilicity and low contact angle. Exposure times ranged from 1 to 180 s. Surface energy gradient slides were characterized by water contact angles obtained using a Krüss G2 contact angle measuring system (Matthews, NC). Gradients were used within 24 h of fabrication because they degraded with time. For example, the standard deviations of the water contact angle measurements were 3° after 24 h (Fig. 1a) but doubled or tripled between 3 and 4 d [33].

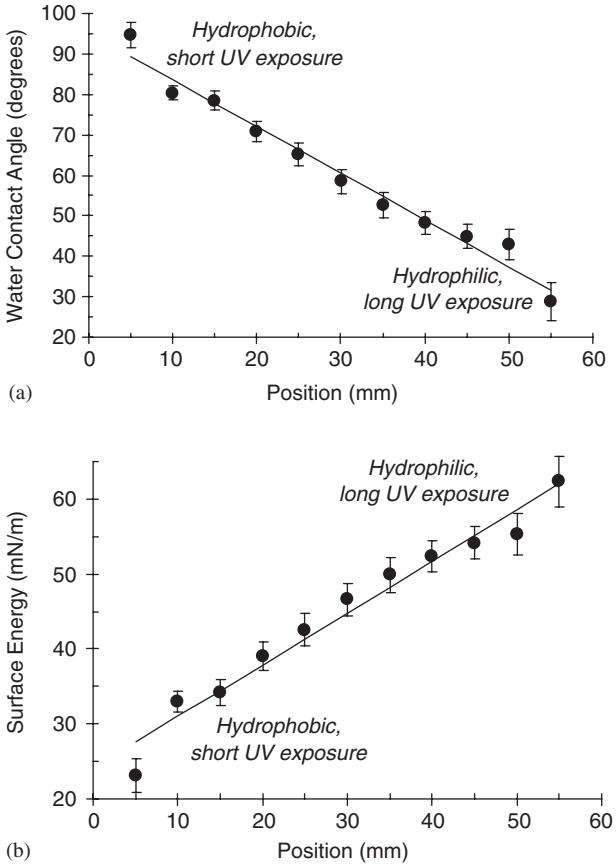

Fig. 1. (a) Water contact angle as a function of position along the surface energy gradients is shown. (b) Water contact was converted to surface energy as described [30] and plotted against position. For both plots (a–b), "*n*" equals 20 for each point and error bars are standard deviation. Lines were fit by linear regression and the Pearson correlation coefficients (*R*) were 0.988 for (a) and 0.983 for (b).

2.3. Fibronectin coating of surface energy gradients

Gradient slides were immersed in a solution of human fibronectin (5 μg/mL; Chemicon International, Inc., Temecula, CA) in phosphate buffered saline (PBS) at room temperature for 30 min. Slides were then rinsed once with PBS and immersed in a 0.1% (by mass) solution of bovine serum albumin (BSA, Sigma, Inc., St. Louis, MO) in PBS at room temperature for 30 min to block non-specific binding. Finally, slides were rinsed once with α modification of Eagle's Minimum Essential Medium (α-MEM, Biowhittaker, Inc., Walkersville, MD) and immediately seeded with cells.

2.4. Cell culture

Established protocols for the culture and passage of MC3T3-E1 cells were followed [34]. Cells were obtained from Riken Cell Bank (Hirosaka, Japan) and cultured in flasks (75 cm^2) at 37 °C in a fully humidified atmosphere at 5% (by volume) CO_2 in α-MEM supplemented with 10% (by volume) fetal bovine serum (Gibco, Rockville, MD) and kanamycin sulfate (60 mg/mL, Sigma, Inc., St. Louis, MO). Media was changed twice weekly and cultures were passaged once per week with 0.25% (by mass)

trypsin and 1 mmol/L EDTA (Gibco, Rockville, MD). For seeding samples, 3 culture flasks (75 cm^2) of 80% confluent MC3T3-E1 cells were trypsinized, washed and suspended in fresh media. Sixty thousand cells diluted into 20 mL of media were added to bacteriological grade polystyrene Petri dishes (85 mm dia.) containing the gradient slides and given 30 min to attach before being moved to the incubator. Cell seeding was more even and uniform if given 30 min to form initial attachments. Twenty surface energy gradient slides were prepared and seeded with cells yielding 4 gradients for each of 5 time points: 8, 24, 64, 136 and 336 h. Media was changed every 48 h. At the indicated time points, gradients were fixed with paraformaldehyde and stained.

2.5. Fixing and staining cells

Cells on gradients (8, 24, 64 and 136 h) were fixed for 5 min (0.5% by mass Triton X-100, 4% by mass paraformaldehyde, 5% by mass sucrose, 1 mmol/L $CaCl_2$, 2 mmol/L $MgCl_2$ in PBS, pH 7.4) and post-fixed for 20 min (same as fix but without Triton X-100). Fixed cells were fluorescently stained for 1 h with 6 μmol/L DAPI (4′,6-diamidino-2-phenylindole, dihydrochloride) and 2 μmol/L Texas Red C_2-maleimide (both from Molecular Probes, Eugene, OR) in PBS. DAPI stains cell nuclei blue for cell counting and Texas Red C_2-maleimide stains cell membranes red for determining cell area [35]. Stained cells were mounted with a coverslip in mounting medium containing DAPI (Vectashield, Vector Laboratories, Inc., Burlingame, CA).

2.6. Automated fluorescence microscopy

Cell number and cell area were determined by automated fluorescence microscopy with a Leica DMR 1200 upright microscope equipped with a computer-controlled translation stage (Vashaw Scientific, Inc., Frederick, MD). Image Pro software (Media Cybernetics, Carlsbad, CA) controlled the stage and image acquisition. Gradients were imaged in a 35×60 grid where 35 images were collected on the axis perpendicular to the gradient and 60 images were collected on the axis parallel to the gradient. Two fluorescence images were captured at each grid position: (1) a red channel image for Texas red C_2-maleimide-stained cell bodies; and (2) a blue channel image of DAPI-stained cell nuclei. The red cell body images were used for determining cell area and the blue cell nuclei images were used to determine cell number. Each captured image had an area of 0.347 mm^2 ($10\times$ eyepiece, $10\times$ objective, $100\times$ magnification) and a total area of 7.3 cm^2 was imaged on each gradient.

For analysis, the cell area and cell number data were binned (placed into categories) according to 7 contact angles (30°, 40°, 50°, 60°, 70°, 80° and 90°). As shown in Fig. 3a, each gradient was 60 mm long and the 7 adjacent bins cover the gradient. The two bins on the ends of the gradient (30° and 90°) spanned 5 mm and each one contained a 35×5 "sub-grid". The middle bins of the gradient (40°, 50°, 60°, 70° and 80°) each spanned 10 mm and each contained a 35×10 "sub-grid".

2.7. Image analysis

The number of nuclei present in each of the blue channel images was tabulated using a macro that was written for Image Pro. The macro opened each blue channel image, counted the number of nuclei and recorded the number in a text file. A second macro was written for red channel images and output cell spread area to a text file. This second macro was programmed to exclude cells that were in contact with other cells (> 1 nucleus) and cells touching the edge of the image. The cell number and cell area text files were imported into Microsoft Excel for analysis. Additional details of the image analysis procedure are provided in Fig. 2.

2.8. Notes

Certain equipment and instruments or materials are identified in the paper to adequately specify the experimental details. Such identification does not imply recommendation by the National Institute of Standards and Technology, nor does it imply the materials are necessarily the best available for the purpose.

The 'standard deviation of the mean' is the same as the 'combined standard uncertainty of the mean' for the purposes of this work.

3. Results

3.1. Contact angle

Water contact angles from the 20 gradient slides were averaged and plotted as a function of position (Fig. 1a). Contact angles ranged from 25° to 95°. A line fit by least-squares linear regression (Fig. 1a) had a Pearson correlation coefficient of 0.988. A *t*-test using an "*n*" of 11 (there are 11 data points) concluded that a linear relationship was present [36]: water contact angle decreased as position on the slide increased ($P < 0.0001$). In Fig. 1b, water contact angle was converted to surface energy as described by Roberson et al. [30] using the following equation:

$$\text{S.E.} = 74.5 - 0.372x - 0.00181x^2;$$

where x is the water contact angle (degrees)

Surface energies ranged from 23 to 62 mN/m on the gradients. These data show that our graded UV-exposure technique yields reproducible, linear gradients in surface energy.

3.2. Cell number

MC3T3-E1 osteoblast-like cells were cultured on fibronectin-coated surface energy gradient slides for 8, 24, 64, 136 or 336 h. Cells were fixed at the indicated time points, stained and analyzed with automated fluorescence microscopy. The 336 h gradients could not be analyzed because the cells became confluent and delaminated. Examples of images that were collected by automated fluorescence microscopy and a demonstration of image analysis are shown in Fig. 2. As shown in Fig. 3a, data for cell number and cell area were binned into 7 contact angles (30°, 40°, 50°, 60°, 70°, 80° and 90°). Fig. 3b shows a plot of average cells/mm^2 as a function of culture time for each of the 7 contact angles. For this analysis, 31,500 images were captured and approximately 750,000 cell nuclei were counted. After 8 h, there were no statistically significant differences in the number of cells on the different contact angles as tested by ANOVA with Tukey's multiple comparison test ($P > 0.05$). This result suggests that surface energy did not affect initial, fibronectin-mediated cell adhesion.

At 24 h, cell numbers did not increase over the 8 h values indicating a lag phase in cell growth (Fig. 3b). Cell numbers increased at 64 and 136 h as the cells proliferated. Cells became confluent and detached from all surfaces by 336 h. Fibronectin-mediated cell proliferation was faster on the more hydrophobic (high water contact angle) surfaces than on the hydrophilic surfaces (low water contact angle).

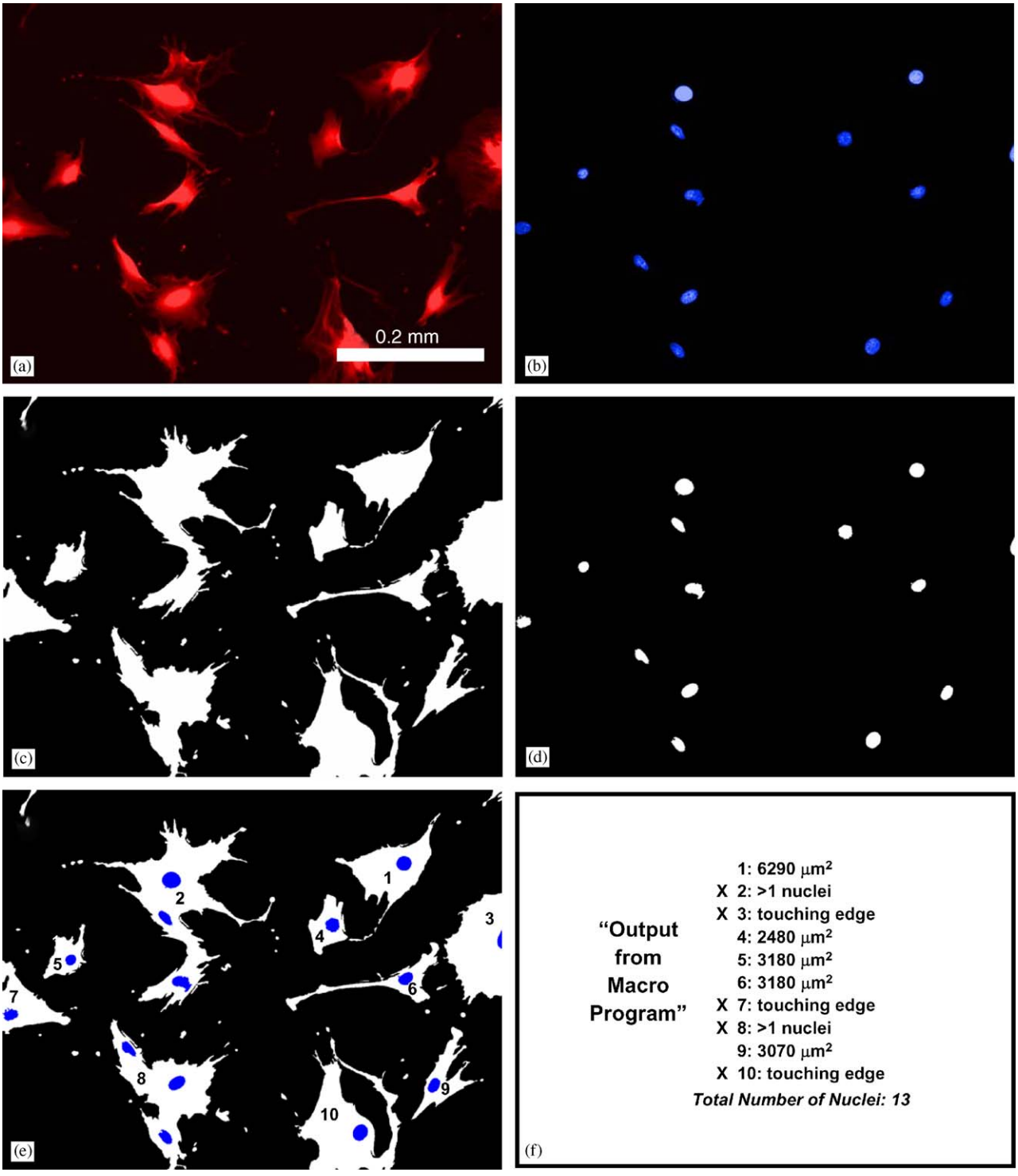

Fig. 2. A demonstration of image capture and analysis is shown. The automated microscope captured a red channel tif image (a: Texas red C_2-maleimide-stained cell bodies) and a blue channel tif image (b: DAPI-stained nuclei) for each field of view. A macro program written for Image Pro software was used for image analysis. The macro opened each blue channel image and counted the number of nuclei as a measure of cell number. For cell area, the macro opened each pair of red and blue images, created masks of the images (c–d) and then merged the images (e). The images were merged so that the number of nuclei per "object" (cell) could be determined. Objects that had more than one nucleus and objects that touched the edge of the image were discarded. Panel (f) shows the output from the macro program and the numbers in (f) correspond to the numbers on the objects in (e). An "X" next to a number in Panel (f) indicates that this object was discarded. Objects 2 and 8 were discarded because they have more than one nucleus. Objects 3, 7 and 10 were discarded because they touch the edge of the image. Objects 1, 4, 5, 6 and 9 lie completely within the image and are not touching any other cells (only one nucleus). Thus the area of these cells was determined and is given in (f). The images in this figure were captured in the middle of a surface energy gradient (60°) after 24 h culture. The size bar in (a) applies to all panels.

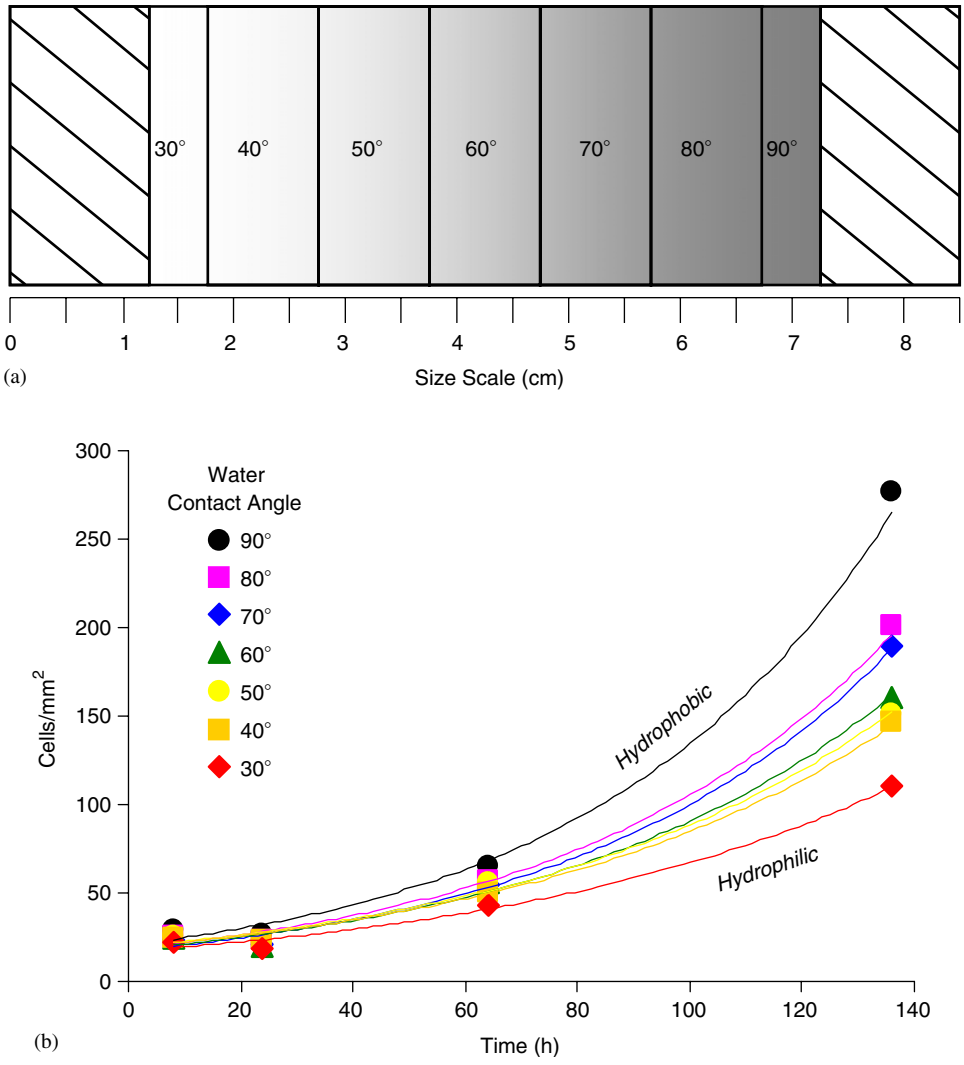

Fig. 3. (a) A diagram of how the surface energy gradients were binned is shown. The whole construct represents a standard glass slide (25 mm × 85 mm) drawn to scale. The crosshatched areas on each end were ignored. The gradient in gray color represents the gradient in surface energy. The boxes labeled 30°, 40°, 50°, 60°, 70°, 80° and 90° indicate the 7 bins that were assigned for each water contact angle. (b) The average number of cells/cm^2 as a function of culture time for different water contact angles is shown. For data points at 8, 24 and 64 h, "*n*" equals 4. For the 136 h data points, "*n*" equals 3 because one specimen was lost. Error bars were omitted for clarity but the standard deviation of the mean averaged 4, 2, 6 and 51 cells/mm^2 for 8, 24, 64 and 136 h, respectively. The log plots are included only as an aid to the eye and were not used for analysis.

Doubling time for cell division was calculated using the 24, 64 and 136 h cell number data. The 8 h cell data was not included in the doubling time analysis so that the lag phase would not influence the calculations. Doubling times were determined by plotting the natural log of the cell count versus time. Plots were fit by least squares linear regression and doubling times were calculated by the following equation: doubling time = ln (2)(1/slope).

The doubling times were plotted against water contact angle (Fig. 4) and the plot was fit by linear regression. The slope of the linear fit indicated that the fibronectin-mediated doubling time decreased by 2 h for every 10° increase in contact angle. The Pearson correlation coefficient of fit was 0.987. Using an "*n*" of 7 (7 data points in the plot) a *t*-test determined that a linear relationship was present [36]: fibronectin-mediated cell doubling time decreased as water contact angle increased ($P < 0.0001$).

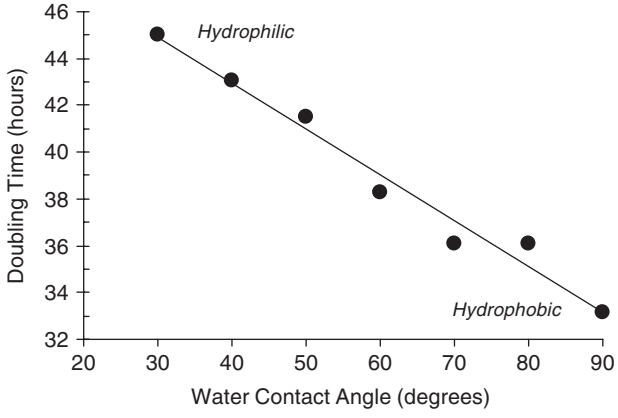

Fig. 4. Fibronectin-mediated cell doubling time as a function of contact angle is shown. The line is fit by linear regression and the Pearson correlation coefficient is 0.987. Fibronectin-mediated doubling time decreased by 2.0 h for every 10° increase in water contact angle.

These data show that fibronectin-mediated cell proliferation was faster on hydrophobic surfaces than on hydrophilic surfaces. These data also demonstrate a linear relationship between rate of fibronectin-mediated cell proliferation and surface energy where doubling time decreased 2 h per 10° increase in contact angle.

3.3. Cell area

Since cell morphology is related to cell function [37,38], cell area was determined on the 8 and 24 h gradients. Cell area could not be determined on the 64 and 136 h gradients because the cells had proliferated and were in contact with one another. Average cell area at 8 and 24 h is plotted against water contact angle in Fig. 5. For this analysis, 16,800 images were captured and the area of approximately 50,000 cells was determined. The data for both 8 and 24 h produced a smooth arc with a maximum at a contact angle of 60°. In general, cells were well spread on all regions of the gradients and had a morphology and spread area comparable to cells cultured on glass slide controls [11].

Pair wise comparisons of the 8 and 24 h data at each contact angle using *t*-test did not yield any statistically significant differences ($P > 0.05$). Thus, there is not a significant difference in fibronectin-mediated cell spreading between 8 and 24 h at each specific contact angle. However, when the cell area at each contact angle for 8 h was compared to cell area at the other contact angles for 8 h using ANOVA with Tukey's test for multiple comparisons, the cell area at 30° was determined to be significantly smaller ($P < 0.05$) than the cell area at 5 of the other 6 contact angles. Likewise, when the cell area at each contact angle for 24 h was compared to cell area at the other contact angles for 24 h using ANOVA with Tukey's test for multiple comparisons, the cell area at 30° was determined to be significantly smaller ($P < 0.05$) than the cell area at 5 of the other 6 contact angles. These results show that the fibronectin-mediated cell spread area on the most hydrophilic part of the gradient (low contact angle) was approximately 25% smaller than on the rest of the gradient.

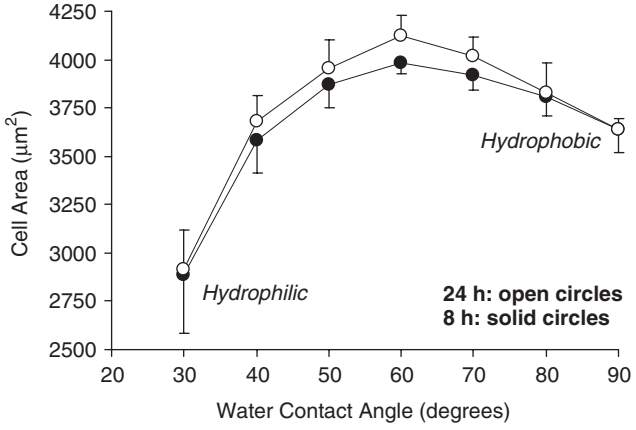

Fig. 5. Fibronectin-mediated mean cell area as a function of contact angle after 8 h (solid) and after 24 h (open) is shown. For each data point, "*n*" equals 4. Error bars are standard deviation of the mean. Only the top (24 h) or bottom (8 h) error bar on each point is shown for clarity. The lines connecting the data points are also only for clarity. A statistical analysis of these results is presented in the "Results" section of the text.

4. Discussion

Several methods for fabricating surface energy gradients employing a variety of surface chemistries have been demonstrated [20,30,39–45]. The advantages and disadvantages of each approach have been reviewed [45]. We chose the method of Roberson et al. [30] because it is quick, simple and inexpensive and because it yields reproducible, linear gradients in surface energy (Fig. 1) [30]. The Roberson et al. [30] method is also versatile as it can be applied to SAMs as well as polymers [44]. In addition, the OH and COOH groups created by ozonolysis in the Roberson et al. [30] method could be used to attach bioactive side chains such as peptides in a defined orientation and in a gradient. These gradient peptide libraries could be used to screen the effect of peptide surface density on cell function. A potential disadvantage of the Roberson et al. [30] approach is that surface chemistry can be difficult to control since ozonolysis yields a mix of hydrophilic species (OH and COOH).

We have combined surface energy gradients with cell culture and automated fluorescence microscopy to yield a combinatorial approach for screening cell response to surface energy. For the current study, 48,300 images were collected, 750,000 cells were counted and 50,000 cells were sized. These large data sets enable the generation of more precise conclusions. A number of previous reports examined cell function on surface energy gradients [20–26,28] but the data collection was not as rigorous as the current study.

Previous studies have examined the effect of surface energy on cell functions such as adhesion, adhesion strength, morphology, spread area, proliferation and differentiation. Both discrete specimens and surface energy gradients were used in these studies and many different outcomes have been observed. In some cases, cell functions are enhanced on hydrophilic surfaces [12,17,20,23,27,28]. In other cases, cell functions are enhanced on hydrophobic surfaces [21,23–26] (the cell proliferation data in the current study). While in other cases, surface energy has no effect on cell functions [20,23] (the cell adhesion data in the current study) or cell functions have a maximum at an intermediate surface energy [16,22,23] (the cell area data in the current study). This wide range of outcomes is possibly a result of the wide variability in experimental conditions such as cell types, incubation times, culture conditions, surface chemistries and surface topography. One firm conclusion from these investigations is that surface energy can influence cell function.

Protein adsorption appears to be a dominant player in dictating cell response to a material and is likely responsible for the wide range of cell responses to surface energy cited above [12,16,17,20–28]. When a biomaterial contacts blood, plasma proteins immediately adsorb onto its surface [46]. Human plasma contains 1175 different proteins [47] and it appears that each unique material will adsorb its own unique subset of these proteins [27,46]. In addition, protein conformation can change upon adsorption and can vary with the time of adsorption [48]. When a cell adheres to a surface, it sees this adsorbed protein layer and not the material itself. Thus, the types, amounts and conformations of adsorbed proteins can dictate cell response to a biomaterial [15,49].

Surface energy is a fundamental material property that can affect protein adsorption. Low surface energy and hydrophobicity generally correlate with increased protein adsorption, increased conformational changes in the adsorbed proteins and irreversible protein adsorption [50]. Protein adsorption to surface energy gradients follows the trend that adsorption amounts are higher on hydrophobic surfaces than on hydrophilic surfaces [39,41]. Thus, the effects of surface energy on cell response observed in previous studies [12,16,17,20–28] were likely an indirect effect where surface energy dictated protein adsorption and conformation which subsequently dictated cell response.

In the current study, surface energy gradients were precoated with fibronectin, blocked with BSA and then exposed to fetal bovine serum during cell culture. Since fibronectin can adsorb irreversibly from serum to surfaces with a range of surface energies [49], it is likely that fibronectin was the predominant surface-adsorbed protein in our studies. Thus, the effects of surface energy on cell response observed in the current study are likely an indirect result of surface energy dictating *fibronectin* adsorption and conformation which subsequently influenced cell response. In addition, since hydrophobicity generally correlates with increased protein adsorption [50], it is possible that we observed increased cell proliferation on the hydrophobic regions of the gradients because more fibronectin adsorbed to the hydrophobic regions during the fibronectin-precoating step.

5. Conclusions

We have combined automated fluorescence microscopy with surface energy gradient technology to examine the effect of surface energy on fibronectin-mediated cell adhesion, spreading and proliferation. The gradient specimens enabled a large range of water contact angles (25–95°) to be tested on each slide and automated microscopy enabled the collection and analysis of large data sets (48,300 images collected and analyzed). Fibronectin-mediated adhesion after 8 h was equal on all regions of the surface energy gradients. Fibronectin-mediated proliferation was faster on the hydrophobic regions of the gradients and had a linear dependence on surface energy. There was a 2.0 h decrease in cell doubling time for every 10° increase in contact angle. Fibronectin-mediated cell spreading was unaffected by changes in surface energy over the majority of the gradient although cells were significantly smaller on the most hydrophilic region (30° water contact angle). The development of this combinatorial approach for probing the fundamental correlations between cell response and surface energy establishes a unique tool for accelerating biomaterials research.

Acknowledgments

We thank Dr. Nathan D. Gallant for insightful suggestions. NRW and SBK acknowledge support from the NRC/NIST post-doctoral fellowship program. This work was funded by NIST and NIH/NIDCR (Y1-DE-1021).

References

[1] Lysaght MJ, Nguy NAP, Sullivan K. An economic survey of the emerging tissue engineering industry. Tissue Eng 1998;4:231–8.
[2] Lysaght MJ, Hazlehurst AL. Tissue engineering: the end of the beginning. Tissue Eng 2004;10:309–20.
[3] Maier WF, Kirsten G, Orschel M, Wei P-A, Holzwarth A, Klein J. Combinatorial chemistry of materials, polymers, and catalysts. In: Malhotra R, editor. Combinatorial materials development. USA: American Chemical Society; 2002. p. 1–3.
[4] Dooley CT, Chung NN, Wilkes BC, Schiller PW, Bidlack JM, Pasternak GW, et al. An all D-amino-acid opioid peptide with central analgesic activity from a combinatorial library. Science 1994;266:2019–22.
[5] Rohrer SP, Birzini ET, Mosley RT, Berk SC, Hutchins SM, Shen D-M, et al. Rapid identification of subtype-selective agonists of the somatostatin receptor through combinatorial chemistry. Science 1998;282:737–40.
[6] Brocchini S, James K, Tangpasuthadol V, Kohn J. Structure–property correlations in a combinatorial library of degradable biomaterials. J Biomed Mater Res 1998;42:66–75.
[7] Meredith JC, Sormana J-L, Keselowsky BG, García AJ, Tona A, Karim A, et al. Combinatorial characterization of cell interactions with polymer surfaces. J Biomed Mater Res 2003;66A:483–90.
[8] Amis EJ. Combinatorial materials science: reaching beyond discovery. Nature Mater 2004;3:83–5.
[9] Anderson DG, Levenberg S, Langer R. Nanoliter-scale synthesis of arrayed biomaterials and application to human embryonic stem cells. Nature Biotech 2004;22:863–6.
[10] Washburn NR, Yamada KM, Simon Jr CG, Kennedy SB, Amis EJ. High-throughput investigation of osteoblast response to crystalline polymers: influence of nanometer-scale roughness on proliferation. Biomaterials 2004;25:1215–24.
[11] Simon Jr CG, Eidelman N, Deng Y, Kennedy SB, Sehgal A, Khatri CA, et al. Combinatorial screening of cell proliferation on poly(L-lactic acid)/poly(D,L-lactic acid) blends. Biomaterials 2005;26:6906–15.
[12] van der Valk P, van Pelt AWJ, Busscher HJ, de Jong HP, Wildevuur CRH, Arends J. Interaction of fibroblasts and polymer surfaces: relationship between surface free energy and fibroblast spreading. J Biomed Mater Res 1983;17:807–17.
[13] Gray DS, Tien J, Chen CS. Repositioning of cells by mechanotaxis on surfaces with micropatterned Young's modulus. J Biomed Mater Res 2003;66A:605–14.

[14] Flemming RG, Murphy CJ, Abrams GA, Goodman SL, Nealey PF. Effects of synthetic micro- and nano-structured surfaces on cell behavior. Biomaterials 1999;20:573–88.
[15] Keselowsky BG, Collard DM, García AJ. Surface chemistry modulates fibronectin conformation and directs integrin binding and specificity to control cell adhesion. J Biomed Mater Res 2003;66A:247–59.
[16] van Wachem PB, Beugeling T, Feijen J, Bantjes A, Detmers JP, van Aken WG. Interaction of cultured human endothelial cells with polymeric surfaces of different wettabilities. Biomaterials 1985;6:403–8.
[17] Schakenraad JM, Busscher HJ, Wildevuur CRH, Arends J. The influence of substratum surface free energy on growth and spreading of human fibroblasts in the presence and absence of serum proteins. J Biomed Mater Res 1986;20:773–84.
[18] Bourassa S, Benjamin WJ. Clinical findings correlated with contact angles on rigid gas permeable contact lens surfaces in vivo. J Am Optometr Assoc 1989;60:584–90.
[19] Lam KH, Schakenraad JM, Groen H, Esselbrugge H, Dijkstra PJ, Feijen J, et al. The influence of surface morphology and wettability on the inflammatory response against poly(L-lactic acid): a semi-quantitative study with monoclonal antibodies. J Biomed Mater Res 1995;29:929–42.
[20] Ruardy TG, Schakenraad JM, van der Mei HC, Busscher HJ. Adhesion and spreading of human skin fibroblasts on physicochemically characterized gradient surfaces. J Biomed Mater Res 1995;29:1415–23.
[21] Lee JH, Jeong BJ, Lee HB. Plasma protein adsorption and platelet adhesion onto comb-like gradient surfaces. J Biomed Mater Res 1997;34:105–14.
[22] Lee JH, Lee JW, Khang G, Lee HB. Interaction of cells on chargeable functional group gradient surfaces. Biomaterials 1997;18:351–8.
[23] Ruardy TG, Moorlag HE, Schakenraad JM, van Der Mei HC, Busscher HJ. Growth of fibroblasts and endothelial cells on wettability gradient surfaces. J Colloid Interf Sci 1997;188:209–17.
[24] Lee JH, Khang G, Lee JW, Lee HB. Platelet adhesion onto chargeable functional group gradient surfaces. J Biomed Mater Res 1998;40:180–6.
[25] Redey SA, Razzouk S, Rey C, Bernache-Assollant D, Leroy G, Nardin M, et al. Osteoclast adhesion and activity on synthetic hydroxyapatite, carbonated hydroxyapatite and natural calcium carbonate: relationship to surface energies. J Biomed Mater Res 1999;45:140–7.
[26] Lee JH, Lee SJ, Khang G, Lee HB. The effect of fluid shear stress on endothelial cell adhesiveness to polymer surfaces with wettability gradient. J Colloid Interf Sci 2000;230:84–90.
[27] Hallab NJ, Bundy KJ, O'connor K, Moses RL, Jacobs JJ. Evaluation of metallic and polymeric biomaterial surface energy and surface roughness characteristics for directed cell adhesion. Tissue Eng 2001;7:55–71.
[28] Lee SJ, Khang G, Lee YM, Lee HB. The effect of surface wettability on induction and growth of neurites from the PC-12 cell on a polymer surface. J Colloid Interf Sci 2003;259:228–35.
[29] Sehgal A, Karim A, Stafford C, Fasolka M. Techniques for combinatorial and high-throughput microscopy part 1: gradient specimen fabrication for polymer thin film research. Microscopy Today 2003;September–October 26–29.
[30] Roberson SV, Fahey AJ, Sehgal A, Karim A. Multifunctional ToF-SIMS: combinatorial mapping of gradient energy substrates. Appl Surf Sci 2002;200:150–64.
[31] Hynes RO, Yamada KM. Fibronectins: multifunctional modular glycoproteins. J Cell Biol 1982;95:369–77.
[32] García AJ, Vega MD, Boettiger D. Modulation of cell proliferation and differentiation through substrate-dependent changes in fibronectin conformation. Mol Cell Biol 1999;10:785–98.
[33] Julthongpiput D, Fasolka MJ, Zhang W, Nguyen T, Amis EJ. Gradient chemical micropatterns: a reference substrate for surface nanometrology. Nano Letters 2005;5:1535–40.
[34] Simon Jr CG, Khatri CA, Wight SA, Wang FW. Preliminary report on the biocompatibility of a moldable, resorbable, composite bone graft consisting of calcium phosphate cement and poly(lactide-*co*-glycolide) microspheres. J Orthopaed Res 2002;20:473–82.
[35] Elliott JT, Tona A, Woodward JT, Jones PL, Plant AL. Thin films of collagen affect smooth muscle cell morphology. Langmuir 2003;19:1506–14.
[36] Glantz SA. Primer of biostatistics, 4th ed. New York: McGraw-Hill; 1997. p. 232.
[37] Folkman J, Moscona A. Role of cell shape in growth control. Nature 1978;273:345–9.
[38] Chen CS, Mrksich M, Huang S, Whitesides GM, Ingber DE. Geometric control of cell life and death. Science 1997;276:1425–8.
[39] Elwing H, Welin S, Askendal A, Nilsson U. Lundström. A wettablity gradient method for studies of macromolecular interactions at the liquid/solid interface. J Colloid Interf Sci 1987;119:203–10.
[40] Pitt WG. Fabrication of a continuous wettability gradients by radio frequency plasma discharge. J Colloid Interf Sci 1988;133:223–7.
[41] Gölander CK, Caldwell K, Lin Y-S. A new technique to prepare gradient surfaces using density gradient solutions. Colloid Surf 1989;42:165–72.
[42] Chaudhury MK, Whitesides GM. How to make water run uphill. Science 1992;256:1539–41.
[43] Lee JH, Kim HG, Khang GS, Lee HB, Jhon MS. Characterization of wettability surfaces prepared by corona discharge treatment. J Colloid Interf Sci 1992;151:563–70.
[44] Roberson S, Sehgal A, Fahey A, Karim A. Time-of-flight secondary ion mass spectrometry (TOF-SIMS) for high-throughput characterization of biosurfaces. Appl Surf Sci 2003;203–204:855–8.
[45] Ruardy TG, Schakenraad JM, van der Mei HC, Busscher HJ. Preparation and characterization of chemical gradient surfaces and their application for the study of cellular interaction phenomena. Surf Sci Rep 1997;29:1–30.
[46] Horbett TA. Protein adsorption on biomaterials. In: Cooper SL, Peppas NA, editors. Biomaterials: interfacial phenomena and applications. Washington, DC: American Chemical Society; 1982. p. 233–44.
[47] Anderson NL, Polanski M, Pieper R, Gatlin T, Tirumalai RS, Conrads TP, et al. The human plasma proteome. Mol Cell Proteomics 2004;3:311–26.
[48] Soderquist ME, Walton AG. Structural changes in proteins adsorbed on polymer surfaces. J Colloid Interf Sci 1980;75:386–97.
[49] Jenney CR, Anderson JM. Adsorbed serum proteins responsible for surface dependent human macrophage behavior. J Biomed Mater Res 2000;49:435–47.
[50] Walton AG, Koltisko B. Protein structure and the kinetics of interactions with surfaces. In: Cooper SL, Peppas NA, editors. Biomaterials: interfacial phenomena and applications. Washington, DC: American Chemical Society; 1982. p. 245–64.